

PARTICLE PRODUCTION FROM SIS TO SPS ENERGIES

W. CASSING

Institut für Theoretische Physik, Heinrich-Buff-Ring 16,

D-35392 Giessen, Germany

E-mail: cassing@theorie.physik.uni-giessen.de

Abstract

The production and propagation of mesons ($\pi, \eta, \rho, \omega, \Phi, K, \bar{K}, J/\Psi$) in proton-nucleus and nucleus-nucleus collisions from 1 - 200 GeV/u is studied within the covariant transport approach HSD, which explicitly allows to investigate selfenergy effects of the hadrons at finite baryon density. Whereas the experimental pion and K^+ spectra can be described without introducing any selfenergies for the mesons, the K^- yield in Ni + Ni collisions is underestimated by a factor of 5–7 at 1.66 and 1.85 GeV/u. However, introducing density dependent antikaon masses in line with effective chiral Lagrangians a satisfactory agreement with the data is achieved. A dropping of the ρ -meson mass with baryon density, as suggested by QCD sumrule studies, is proposed to explain the dilepton spectra for S + Au and Pb + Au at SPS energies, which indicates independently that a partial restoration of chiral symmetry might be found already in the present experiments.

1 Introduction

The study of hot and dense nuclear matter via relativistic nucleus-nucleus collisions is the major aim of high energy heavy-ion physics. Nowadays, the search for a restoration of chiral symmetry at high baryon density or for a phase transition to the quark-gluon plasma (QGP) is of specific interest. However, any conclusions about the hadron properties at high temperature or baryon densities must rely on the comparison of experimental data with theoretical approaches based on nonequilibrium kinetic theory. Among these, the covariant RBUU approach [1, 2], the QMD [3] or RQMD model [4], and the HSD approach [5] have been successfully used in the past. As a genuine feature of transport theories there are two essential ingredients: i.e. the baryon (and meson) scalar and vector selfenergies – which are neglected in many approaches – as well as in-medium elastic and inelastic cross sections for all hadrons involved.

Selfenergy effects in the production of particles have been found so far for antiprotons at SIS energies [6, 7], though the actual magnitude of the attractive \bar{p} -potential in the nuclear medium is still a matter of debate since the strong \bar{p} annihilation with nucleons is not sufficiently under control. As advocated in Refs. [8, 9, 10, 11] on the

basis of effective chiral Lagrangians also antikaons should feel strong attractive forces in the medium so that their production threshold should be reduced at finite baryon density. The vector mesons ρ and ω , furthermore, are expected to drop in mass with baryon density according to QCD sumrule studies [12], which is basically a consequence of the dropping scalar quark condensate $\langle \bar{q}q \rangle$ with the quark density $\langle q^\dagger q \rangle$ [13]. Whereas a direct enhancement of the ρ -meson yield is hard to observe experimentally due to the short lifetime of the ρ and the strong final state interactions of the pions, dilepton spectroscopy is expected to provide valuable information on the ρ spectral function in the dense medium.

The present article is organized as follows: Section 2 contains a brief description of the transport approach employed as well as a specification of the meson selfenergies incorporated in the calculation. Section 3 is devoted to a presentation of the calculated results for π , K^+ , and K^- spectra in comparison to available data at SIS, AGS and SPS energies. Section 4 concentrates on dilepton physics at SPS energies while Section 5 concludes this study with a summary and discussion of open problems.

2 Ingredients of the transport approach

In this work the dynamical analysis of p+A and A+A reactions is performed within the HSD¹ approach [5] which is based on a coupled set of covariant transport equations for the phase-space distributions $f_h(x, p)$ of hadron h [2, 5], i.e.

$$\begin{aligned} & \left\{ \left(\Pi_\mu - \Pi_\nu \partial_\mu^p U_h^\nu - M_h^* \partial_\mu^p U_h^S \right) \partial_x^\mu + \left(\Pi_\nu \partial_\mu^x U_h^\nu + M_h^* \partial_\mu^x U_h^S \right) \partial_p^\mu \right\} f_h(x, p) \\ &= \sum_{h_2 h_3 h_4 \dots} \int d^2 d^3 d^4 \dots [G^\dagger G]_{12 \rightarrow 34 \dots} \delta^4(\Pi + \Pi_2 - \Pi_3 - \Pi_4 \dots) \\ & \times \left\{ f_{h_3}(x, p_3) f_{h_4}(x, p_4) \bar{f}_h(x, p) \bar{f}_{h_2}(x, p_2) \right. \\ & \left. - f_h(x, p) f_{h_2}(x, p_2) \bar{f}_{h_3}(x, p_3) \bar{f}_{h_4}(x, p_4) \right\} \dots \quad . \end{aligned} \quad (1)$$

In Eq. (1) $U_h^S(x, p)$ and $U_h^\mu(x, p)$ denote the real part of the scalar and vector hadron selfenergies, respectively, while $[G^\dagger G]_{12 \rightarrow 34 \dots} \delta^4(\Pi + \Pi_2 - \Pi_3 - \Pi_4 \dots)$ is the 'transition rate' for the process $1 + 2 \rightarrow 3 + 4 + \dots$ which is taken to be on-shell in the semiclassical limit adopted. The hadron quasi-particle properties in (1) are defined via the mass-shell constraint [2],

$$\delta(\Pi_\mu \Pi^\mu - M_h^{*2}) \quad , \quad (2)$$

with effective masses and momenta (in local Thomas-Fermi approximation) given by

$$\begin{aligned} M_h^*(x, p) &= M_h + U_h^S(x, p) \\ \Pi^\mu(x, p) &= p^\mu - U_h^\mu(x, p) \quad , \end{aligned} \quad (3)$$

while the phase-space factors

$$\bar{f}_h(x, p) = 1 \pm f_h(x, p) \quad (4)$$

¹Hadron String Dynamics

are responsible for fermion Pauli-blocking or Bose enhancement, respectively, depending on the type of hadron in the final/initial channel. The dots in Eq. (1) stand for further contributions to the collision term with more than two hadrons in the final/initial channels. The transport approach (1) is fully specified by $U_h^S(x, p)$ and $U_h^\mu(x, p)$ ($\mu = 0, 1, 2, 3$), which determine the mean-field propagation of the hadrons, and by the transition rates $G^\dagger G \delta^4(\dots)$ in the collision term, that describes the scattering and hadron production/absorption rates.

The scalar and vector mean fields U_h^S and U_h^μ for baryons are taken from Ref. [5] and don't have to be specified here again. The pions and η 's as Goldstone bosons are expected not to change their properties in the medium; they will be treated as bare particles throughout all calculations. Furthermore, the K^+ meson energy changes only very moderately with baryon density according to Kaplan and Nelson [10, 14, 15] due to a partial cancellation of the scalar and vector kaon selfenergies. Thus, they are also produced and propagated as free particles. The antikaon and vector meson potentials in the medium, however, have to be specified more explicitly.

2.1 K^- , ρ , ω , Φ selfenergies

As in case of antiprotons there are a couple of models for the antikaon and vector meson selfenergies which differ in the actual magnitude of the meson potential. Without going into a detailed discussion of the various approaches we adopt the more practical point of view, that the actual K^- , ρ , ω and Φ selfenergies are unknown and as a guide for our analysis use a linear extrapolation of the form (for the meson x),

$$m_x^*(\rho_B) = m_x^0 \left(1 - \alpha_x \frac{\rho_B}{\rho_0} \right) \geq m_q + m_{\bar{q}}, \quad (5)$$

with $\alpha_x \approx 0.2$ for antikaons, which leads to a fairly reasonable reproduction of the antikaon mass from Refs.[10, 14] and the recent results from Waas, Kaiser and Weise [11], $\alpha_x \approx 0.18$ for ρ and ω mesons according to Hatsuda and Lee [12] and $\alpha_x \approx 0.025$ for the Φ meson. We note that the dropping of the meson masses is associated with a corresponding scalar energy density in the baryon/meson Lagrangian, such that the total energy-momentum is conserved during the heavy-ion collision (cf. Ref. [5]).

2.2 Elastic and inelastic reaction channels

Baryon-baryon (BB) collisions are described using free differential cross sections from Ref. [16] for invariant energies $\sqrt{s} \leq 2.6$ GeV and by the LUND string formation and fragmentation model [17] for $\sqrt{s} \geq 2.6$ GeV, which generates the hadronic final states of a BB collision. The same concept is used for meson-baryon (mB) reactions, where for $\sqrt{s} \leq 2.3$ GeV differential cross sections from Ref. [16] are employed whereas the LUND model is used for higher invariant energies. Meson-meson (mm) reactions (e.g. $\pi\pi \rightarrow \rho$, $\pi\rho \rightarrow \Phi$, $\pi\rho \rightarrow a_1$) are described within the Breit-Wigner resonance picture using branching ratios from the nuclear data tables [18]. In all reaction channels the thresholds are shifted according to the actual mass of the hadrons (at finite baryon density $\rho_B = \sqrt{j_\mu j^\mu}$, where $j_\mu(x)$ is the local baryon current). Also within the

Breit-Wigner resonance formation the actual masses of the hadrons are used, whereas their width is corrected according to the local phase space for the decay. For the detailed parametrizations employed (including also baryon-hyperon and meson-hyperon channels) the reader is referred to Refs. [5, 19, 20].

2.3 Optimizing for high baryon density

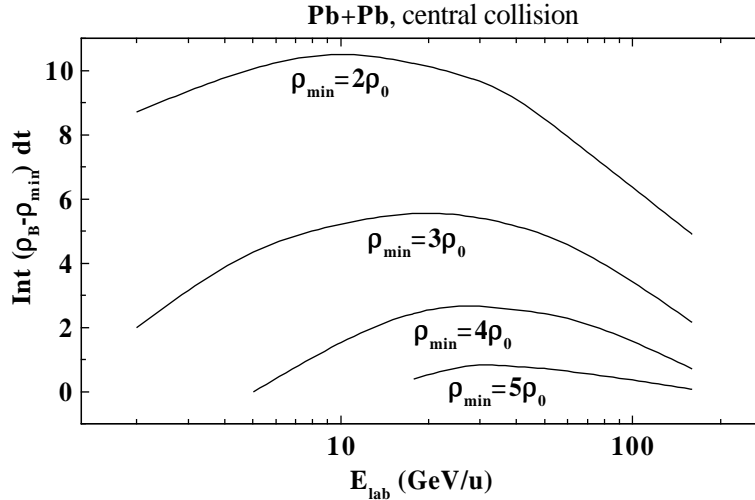


Figure 1: The quantity F (6) for central Pb + Pb collisions as a function of the bombarding energy per nucleon for 4 different cuts in ρ_{min} .

In order to probe the restoration of chiral symmetry at high baryon density in nucleus-nucleus collisions, one has to perform experiments with heavy nuclei (e.g. Pb + Pb) and optimize the beam energy to achieve a large volume of high baryon density for a sufficiently long time. In this respect central collisions of Pb + Pb have been investigated within the transport approach specified above and the 'stopped' baryon density $\rho_b^s(t)$ - including only baryons with rapidity $|y| \leq 0.7$ in the cms - has been computed in a central volume $V = \pi R^3 / \gamma_{CM}$ with $R = 4$ fm, while γ_{CM} is the Lorentz factor in the nucleus-nucleus center-of-mass system. Since we are interested in high baryon densities above some value ρ_{min} for long times, we consider the quantity

$$F = \int dt (\rho_B^s(t) - \rho_{min}) \Theta(\rho_B^s(t) - \rho_{min}), \quad (6)$$

which should serve as a useful guide in the optimization problem. The quantity F (6) is displayed in Fig. 1 for central collisions of Pb + Pb from 1 - 200 GeV/u for different values of ρ_{min} from 2 - 5 ρ_0 ($\rho_0 \approx 0.168 \text{ fm}^{-3}$). Thus optimal bombarding energies for baryon densities above $4\rho_0$ should be around 20 - 30 GeV/u in order to explore the properties of an intermediate phase, where the chiral symmetry might approximately be restored and the hadron masses (except for the Goldstone bosons) might be close to their current quark masses $m_q + m_{\bar{q}}$.

3 Meson production in nucleus-nucleus collisions

3.1 Pions

The pions as the lightest Goldstone bosons are not expected to change their properties in the dense nuclear medium significantly - except in a quark-gluon-plasma (QGP) phase - such that their production and propagation should be reasonably described without introducing any selfenergies. As an example for SIS energies we show in Fig. 2 the calculated results [5] for transverse π^0 spectra in Ar + Ca collisions at 1.5 GeV/u (for $0.68 \leq y_{lab} \leq 0.84$) in comparison to the data of the TAPS collaboration [21] (open squares), which are described over four orders of magnitude with relative deviations of less than 30%. Similar results have been obtained for various systems at 1 - 2 GeV/u in Ref. [19]. Quantitatively similar experiences have been made at AGS energies as can

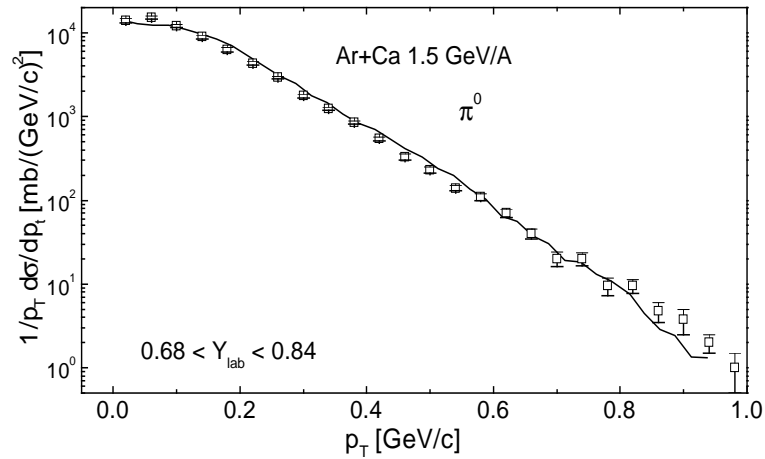


Figure 2: The calculated transverse π^0 spectra (solid line) in Ar + Ca collisions at 1.5 GeV/u (for $0.68 \leq y_{lab} \leq 0.84$) in comparison to the data of the TAPS collaboration[21] (open squares)

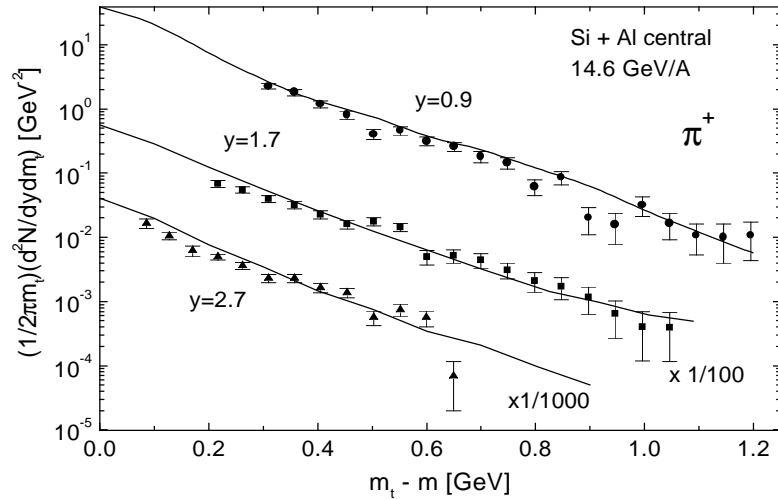


Figure 3: The calculated transverse mass spectra for π^+ (solid lines) in ntral collisions of Si + Al at 14.6 GeV/u for different rapidities in laboratory ($y = 0.9, 1.7, 2.7$) in comparison to the data from Ref. [22].

be extracted from Fig. 3 where the transverse π^+ mass spectra for central collisions of Si + Al at 14.6 GeV/u are displayed for 3 different rapidities in the laboratory system in comparison to the data from Ref. [22].

As an example for the pion yield at SPS energies we show in Fig. 4 the π^- rapidity distribution for central S + S collisions at 200 GeV/u in comparison to the data from Ref. [23] (open squares), which are approximately of Gaussian shape. At midrapidity ($y = 0$) here the π^- density is about a factor of 7 higher than the proton density. This indicates that the available energy is dominantly used for mass production (in form of pions) and that during the longitudinal expansion of the 'hadronic fireball' meson-meson reaction channels should occur more frequent than meson-baryon or baryon-baryon reactions.

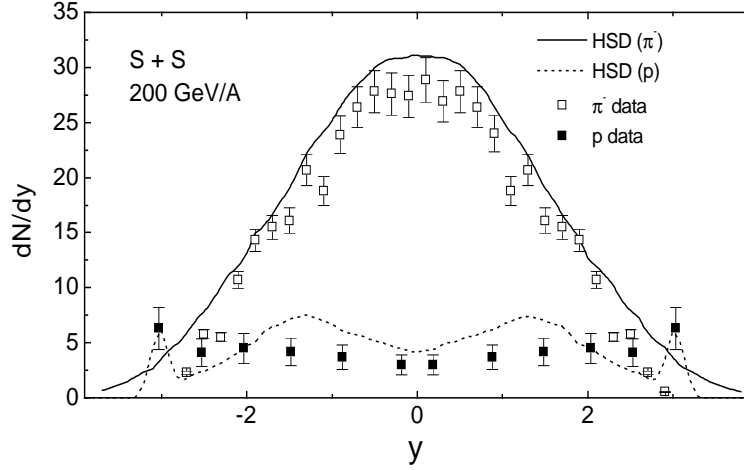


Figure 4: The π^- rapidity distribution (solid line) for central S + S collisions at 200 GeV/u in comparison to the data from Ref. [23] (open squares). The dotted line shows the calculated proton rapidity distribution in comparison to the respective data from Ref. [23] (full squares).

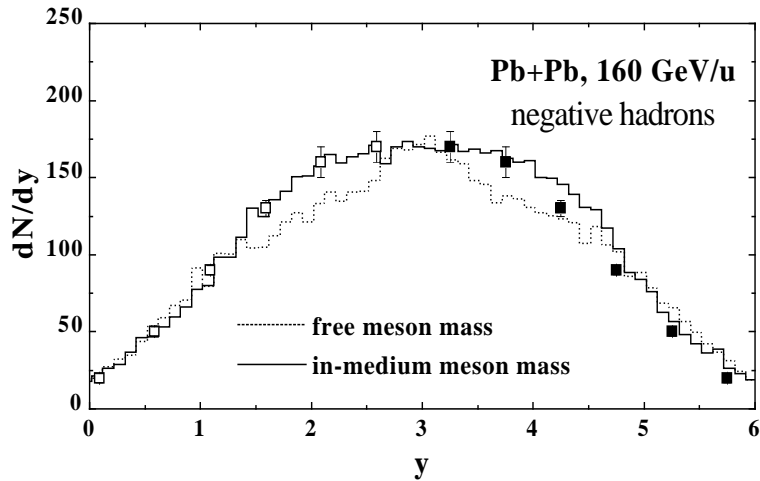


Figure 5: The preliminary rapidity distribution of negative hadrons from NA49 [24] (full squares) in comparison to the HSD results [26]. The solid line corresponds to a calculation (at $b = 2$ fm) including the dropping meson masses from Eq. (5), whereas the dotted line results from a calculation with bare meson masses. The open squares are obtained by reflecting the full squares at midrapidity.

The shape of the pion rapidity distribution is not changed significantly when going over to central collisions of Pb + Pb at 160 GeV/u as can be seen from Fig. 5, where the preliminary rapidity distribution of negative hadrons (essentially π^- , K^- and \bar{p}) from NA49 [24] is shown in comparison to the HSD results [26]. Here the solid line corresponds to a calculation (at $b = 2\text{fm}$) including the dropping meson masses from Eq. (5), whereas the dotted line results from a calculation with bare meson masses. The broadening of the rapidity distribution around midrapidity ($y \approx 3$) in the dropping mass scenario is due to pions from ρ and ω decays, which are produced with a wider distribution in rapidity in this case. Since the proton distribution $dN_p/dy \approx 40 - 45$ at midrapidity (cf. Fig. 22 in Ref. [5]) the π^- to proton ratio is only about 4 for central Pb + Pb collisions such that the baryon density in the expanding 'hadronic fireball' is significantly higher than that for central S + S collisions.

3.2 Kaons and antikaons

Whereas kaons should feel a slightly repulsive potential in the nuclear medium according to the approach by Kaplan and Nelson [10] or Waas, Kaiser and Weise [11], the antikaons should experience a stronger attractive potential at finite baryon density, which is also supported by K^- atomic data [27]. As a first order approximation we thus assume the K^+ potential or selfenergy to be zero and adopt the linear parametrization for the in-medium K^- mass from Eq. (5). For the detailed reaction channels and cross sections considered the reader is referred to Ref. [20].

The l.h.s. of Fig. 6 shows the calculated results for the inclusive K^+ invariant cross section for Ni + Ni collisions at 0.8, 1.0 and 1.8 GeV/u at $\theta_{lab} = 44^\circ$, that have been transformed to the nucleus-nucleus cms, in comparison to the preliminary K^+ spectra from Ref. [28, 29]. Since the data can be described quite reasonably at all energies from 0.8 - 1.8 GeV/u, apparently no selfenergy effects are needed for K^+ mesons. This finding is also in accordance with earlier studies on K^+ production in nucleus-nucleus [30, 31, 32] and proton-nucleus collisions [33]. On the hand, due to the rather stable quasi-particle properties of the kaons in the medium, they qualify as probes in connection with the nuclear-equation-of-state (EOS) as suggested early by Aichelin and Ko [34].

The r.h.s. of Fig. 6 shows the calculated K^- spectra for Ni + Ni at 1.85 GeV/u at 0° with respect to the beam axis in the nucleus-nucleus cms in comparison with the data of Ref. [35] (full squares) and the preliminary data for Ni + Ni at 1.8 GeV/u from Ref. [36] (open dots). The dashed line reflects a calculation including the bare antikaon mass without any antikaon absorption, while the dash-dotted line includes antikaon absorption, which reduces the cross section on average by a factor of 5 for the Ni + Ni system. However, the data are underestimated severely in the bare K^- mass approximation. The solid line in Fig. 6 (r.h.s.) shows the result of a calculation, where the K^- mass drops with baryon density according to Eq. (5) with $\alpha_x = 0.2$ including also antikaon reabsorption². With increasing α_x not only the magnitude

²For practical purposes one should consider α_x to be a free parameter to be fixed in comparison to the experimental data in order to learn about the magnitude of the antikaon selfenergy. In fact, we obtain a much better reproduction of the spectra for $\alpha_x \approx 0.24$, but due to the uncertainties involved in the elementary BB production cross sections one cannot determine this value very reliably.

of the spectrum is increased, but also the slope becomes softer. For $\alpha_x \approx 0.2$ we still underestimate the experimental spectra slightly, but it is clearly seen that quite sizeable antikaon attractive selfenergies are needed to reproduce the data. This finding is also in line with an independent calculation by Li, Ko and Fang [37].

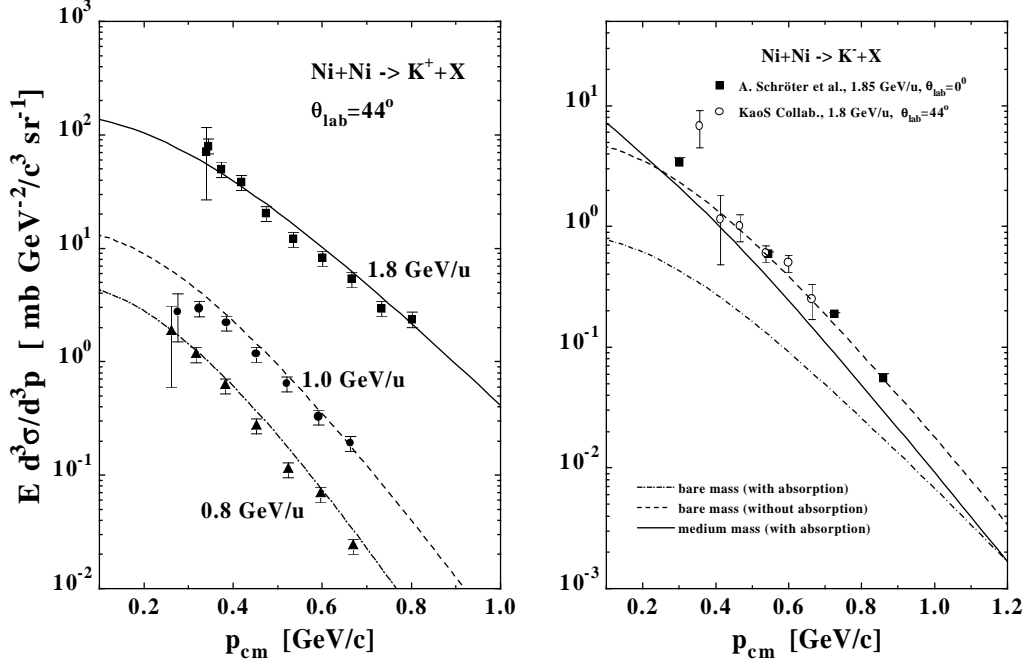


Figure 6: (l.h.s.) The calculated results for the inclusive K^+ invariant cross section for Ni + Ni collisions at 0.8, 1.0 and 1.8 GeV/u at $\theta_{lab} = 44^\circ$, that have been transformed to the nucleus-nucleus cms, in comparison to the preliminary K^+ spectra from Ref. [28, 29]. (r.h.s.) The calculated K^- spectra for Ni + Ni at 1.85 GeV/u at 0° with respect to the beam axis in the nucleus-nucleus cms in comparison with the data of Ref. [35] (full squares) and the preliminary data for Ni + Ni at 1.8 GeV/u from Ref. [36] (open dots). The dashed line reflects a calculation including the bare K^- mass without any antikaon absorption, while the dash-dotted line includes antikaon absorption. The solid line corresponds to a calculation with a dropping antikaon mass according to Eq. (5) for $\alpha_x = 0.2$.

The enhanced production of strangeness is also known from experiments at AGS and SPS energies[38]. As an example Fig. 7 shows the measured K^+/π^+ ratio for pp, Si + Al, Si + Cu, Si + Au and Au + Au at AGS energies [39], which increases by about a factor of 3 with the number of participating nucleons. Whereas a HSD calculation with in-medium meson masses (solid line) [5] approximately reproduces this trend, the same calculation with bare meson masses (lower dotted line) underestimates the K^+/π^+ ratio significantly. The actual enhancement in the dropping mass scenario is due to a large contribution from the channel $meson + meson \rightarrow K^+K^-$, which is enhanced sizeably for a dropping antikaon mass. Differential transverse momentum spectra for kaons and antikaons at midrapidity for central Au + Au collisions at 10.8 GeV/u should shed some further light on this issue. Note, that RQMD calculations [40] for these systems also underestimate the K^+/π^+ ratio by about a factor of 1.5.

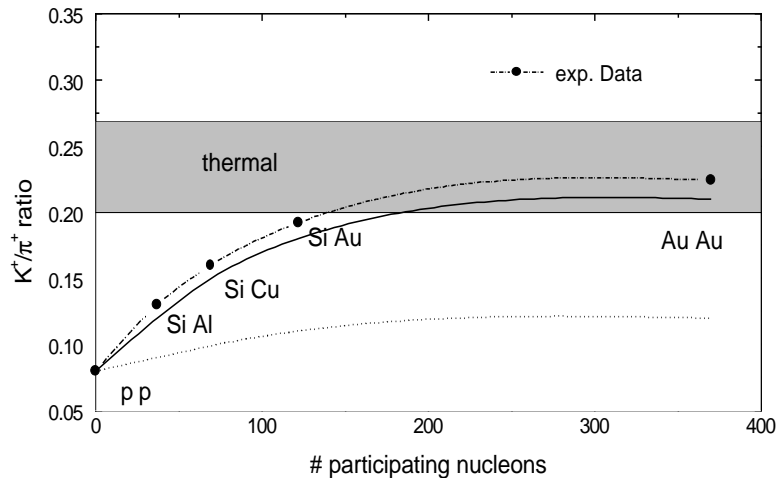


Figure 7: The measured K^+/π^+ ratio for pp, Si + Al, Si + Cu, Si + Au and Au + Au at AGS energies [39] (full dots) in comparison to HSD calculations with in-medium meson masses (solid line) [5] and bare meson masses (lower dotted line).

4 Electromagnetic probes

Photons and dileptons are particularly well suited for an investigation of the violent phases of a high-energy heavy-ion collision because they can leave the reaction volume essentially undistorted by final-state interactions. Whereas the signal from direct photons is largely covered by the electromagnetic decays of light neutral mesons (π^0, η), e^+e^- or $\mu^+\mu^-$ pairs at higher invariant masses do not suffer that much from large background contributions. Indeed, dileptons from heavy-ion collisions have been observed by the DLS collaboration at the BEVALAC [41, 42, 43] and by the CERES [44], HELIOS [45, 46], NA38 [47] and NA50 [48] collaborations at SPS energies.

4.1 e^+e^- pairs

Quite some years ago it has been found within microscopic transport studies at BEVALAC/SIS energies [49] that above about 0.5 GeV of invariant mass (of the lepton pair) the dominant production channel is from $\pi^+\pi^-$ annihilation, such that the properties of the short lived ρ meson could be explored at high baryon density. The data available so far, however, did not allow for a closer distinction of the various models proposed. At SPS energies the enhancement of the low mass dimuon yield in S + W compared to p + W collisions [45] has been first suggested by Koch *et al.* [50] to be due to $\pi^+\pi^-$ annihilation. Furthermore, Li *et al.* [51] have proposed that the enhancement of the e^+e^- yield in S + Au collisions - as observed by the CERES collaboration [44] - should be due to an enhanced ρ -meson production (via $\pi^+\pi^-$ annihilation) and a dropping ρ -mass in the medium. In fact, their analysis - which was based on an expanding fireball scenario in chemical equilibrium - could be confirmed within the HSD transport calculations in Ref. [52]. However, also a more conventional approach including the increase of the ρ -meson width in the medium due to the coupling of the ρ, π, Δ

and nucleon dynamics [53] was found to be roughly compatible with the CERES data. On the other hand, the dimuon data of the HELIOS-3 collaboration[45] could only be described satisfactorily when including dropping meson masses[54]. In the following some more recent results from Refs. [25, 26] are reported, where systematic studies on the various dilepton channels from 10 - 200 GeV/u have been performed.

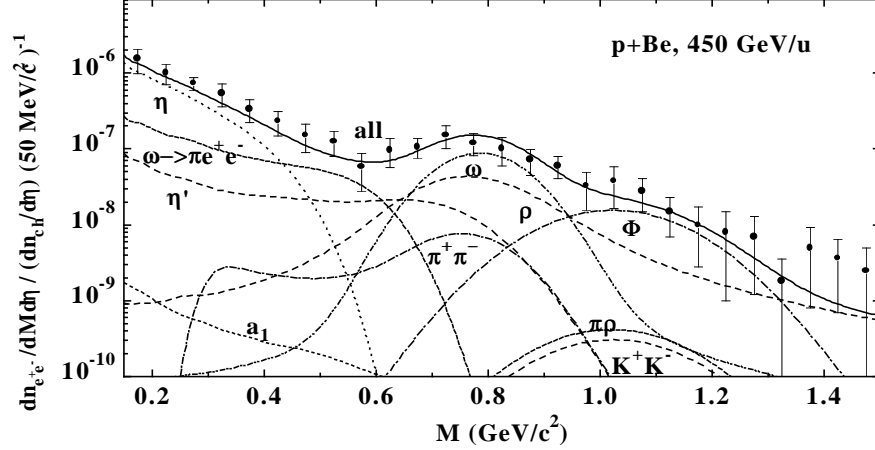


Figure 8: The calculated dilepton spectra (full solid line) for p + Be at 450 GeV/u in comparison with the data from Ref. [44]. The thin lines indicate the individual contributions from the different production channels including the CERES-acceptance and mass resolution.

As an example for dilepton spectra at SPS energies Fig. 8 shows the spectral decomposition as a function of the e^+e^- invariant mass M for p + Be at 450 GeV/c in comparison to the data of the CERES collaboration [44]. In this case the spectrum can be fully accounted for by the electromagnetic decays of the η , η' and vector mesons ρ^0 , ω and Φ . Contributions from meson-meson channels ($\pi^+\pi^-$, K^+K^- , $\pi\rho$) are of minor importance.

The situation changes quite dramatically when going over to nucleus-nucleus collisions. For Pb + Au at 160 GeV/u (and semicentral collisions) the dominant yield for invariant masses $0.3 \text{ GeV} \leq M \leq 0.7 \text{ GeV}$ stems from $\pi^+\pi^-$ annihilation (cf. Fig. 9). Also in the Φ mass regime about 1 GeV there is a large contribution from K^+K^- and $\pi\rho$ annihilation to dileptons for both scenarios: with bare meson masses (upper part of Fig. 9) and with in-medium meson masses (lower part of Fig. 9). Whereas most of the processes (Dalitz and direct decays) occur in the vacuum at zero baryon density, the $\pi\pi \rightarrow \rho^0 \rightarrow e^+e^-$ and direct ρ^0 (from BB and mB collisions) decay still occur at finite baryon density such that a dropping ρ mass also leads to a shift of the respective contribution to lower invariant masses M . In Fig. 9 both scenarios are compared to the preliminary data of the CERES collaboration [55] including the experimental cuts in rapidity y , transverse momentum of the leptons as well as the CERES mass resolution; due to the present statistics, however, there is no unique conclusion since the calculation with bare meson masses (upper part) also describes the data except for one point at 0.6 GeV. On the other hand, the present preliminary data match well with the calculation including the in-medium meson masses. Apart from better statistics also a higher mass resolution of the CERES detector (especially in the ρ , ω , Φ mass regime) should allow to disentangle the different scenarios in the next years.

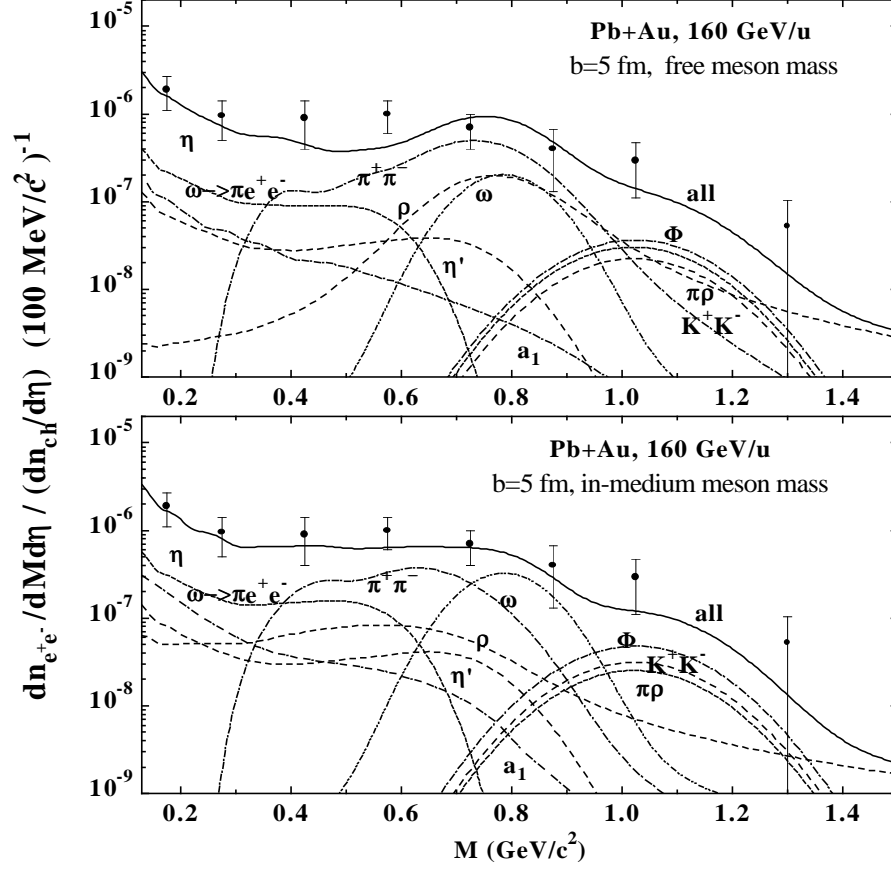


Figure 9: Dilepton invariant mass spectra for semicentral collisions of Pb + Au at 160 GeV/u (full solid lines) in comparison to the preliminary data of the CERES collaboration [55]. The upper part shows the results of a calculation with bare meson masses whereas the lower part includes the dropping meson masses (5).

5 Summary

In this article the production of secondary particles in proton-nucleus and nucleus-nucleus collisions from 1 - 200 GeV/u has been investigated within the covariant transport approach HSD [5]. The analysis shows that π and K^+ spectra are reasonably well described in this energy regime without introducing any medium modifications for these mesons (cf. also Ref. [19] in case of pions). This experience is fully in line with earlier studies on this subject and the results from independent groups [56, 57]. The antikaon spectra, however, are underestimated severely when incorporating only bare kaon masses roughly in line with the study by Li *et al.* [37]. When including an attractive antikaon potential comparable to that proposed by Waas, Kaiser and Weise [11], a satisfactory description of the K^- spectra can be given, both in the actual magnitude as well as in the slope. It is worth noting that the π -hyperon $\rightarrow K^- N$ production channels play a sizeable role in case of the vacuum antikaon mass, whereas their contribution in the 'dropping mass scenario' becomes of minor importance.

The 'observed' dropping of the antikaon mass with baryon density may be inter-

preted as a step towards a partial restoration of chiral symmetry that can already be seen at SIS energies (1 - 2 GeV/u). Similar observations have been made at AGS energies (10 - 15 GeV/u) (cf. Fig. 7) as well as at SPS energies (160 - 450 GeV/u), where especially a dropping of the ρ -mass can be used to accurately describe the dilepton spectra from heavy-ion reactions [52, 51, 54] at invariant masses $0.3 \text{ GeV} \leq M \leq 0.7 \text{ GeV}$. The enhancement of dileptons (about a factor of 3) seen in the Φ mass region is essentially due to the meson-meson production channels $\pi\rho \rightarrow \Phi$ and $K^+K^- \rightarrow \Phi$.

Though there are quite a number of indications for dropping meson masses in the medium by now, one has to properly examine the possibility that conventional many-body effects such as 'resonance-hole' loops [58] may also account for the spectra observed. In addition, detailed experimental studies on K^- , ρ and ω production in proton (pion) - nucleus reactions should be performed close to threshold energies since a 20% reduction of their mass at density ρ_0 should clearly be visible in the respective spectra [59].

Acknowledgments

The author acknowledges valuable and inspiring discussions with A. Drees, V. Metag, P. Senger, H. Specht and Gy. Wolf. Furthermore, he likes to thank his colleagues and collaborators for their help and work, on which many of the results presented in this article are based, in particular E. L. Bratkovskaya, W. Ehehalt, C. M. Ko, U. Mosel, A. Sibirtsev and S. Teis.

References

- [1] W. Cassing and U. Mosel, *Prog. Part. Nucl. Phys.* 25, 235 (1990).
- [2] K. Weber, B. Blättel, W. Cassing *et al.*, *Nucl. Phys. A* 539, 713 (1992).
- [3] J. Aichelin, *Phys. Reports* 202, 233 (1991).
- [4] H. Sorge, H. Stöcker, and W. Greiner, *Ann. Phys.* 192, 266 (1989); *Nucl. Phys. A* 498, 567c (1989); H. Sorge *et al.*, *Z. Phys. C* 47, 629 (1990); *Phys. Lett. B* 243, 7 (1990).
- [5] W. Ehehalt and W. Cassing, *Nucl. Phys. A* 602, 449 (1996).
- [6] S. Teis, W. Cassing, T. Maruyama, and U. Mosel, *Phys. Lett. B* 319, 47 (1993); *Phys. Rev. C* 50, 388 (1994).
- [7] G. Q. Li *et al.*, *Phys. Rev. C* 49, 1139 (1994).
- [8] G. E. Brown *et al.*, *Phys. Rev. C* 43, 1881 (1991).
- [9] G. E. Brown and M. Rho, *Phys. Rev. Lett.* 66, 2720 (1991).
- [10] D. B. Kaplan and A. E. Nelson, *Phys. Lett. B* 175, 57 (1986).

- [11] T. Waas, N. Kaiser, and W. Weise, *Phys. Lett. B* 379, 34 (1996).
- [12] T. Hatsuda and S. Lee, *Phys. Rev. C* 46, R34 (1992).
- [13] U. Vogl and W. Weise, *Prog. Part. Nucl. Phys.* 27, 195 (1991).
- [14] A. E. Nelson and D. Kaplan, *Phys. Lett. B* 192, 193 (1987).
- [15] G. Q. Li and C.M. Ko, *Nucl. Phys. A* 582, 731 (1995).
- [16] Landolt-Börnstein, *New Series*, ed. H. Schopper, I/12 (1988).
- [17] B. Nilsson-Almqvist and E. Stenlund, *Comput. Phys. Commun.* 43, 387 (1987).
- [18] Review of Particle Properties, *Phys. Rev. D* 50 (1994).
- [19] S. Teis, W. Cassing, M. Effenberger *et al.*, nucl-th/9609009, *Z. Phys. A*, in print.
- [20] W. Cassing, E. L. Bratkovskaya, U. Mosel *et al.*, nucl-th/9609050, *Nucl. Phys. A*, in print.
- [21] F. D. Berg *et al.*, *Phys. Rev. Lett.* 72, 977 (1994).
- [22] T. Abbott *et al.*, E802 Coll., *Phys. Rev. C* 50, 1024 (1994).
- [23] H. Stroebele *et al.*, *Nucl. Phys. A* 525, 59c (1991).
- [24] H. Appelshäuser *et al.*, *GSI Annual Report* 1995, p. 54.
- [25] E. L. Bratkovskaya, W. Cassing and U. Mosel, nucl-th/9605025, *Z. Phys. C*, in print.
- [26] E. L. Bratkovskaya and W. Cassing, *preprint* UGI-96-25.
- [27] E. Friedman, A. Gal and C. J. Batty, *Phys. Lett. B* 308, 6 (1993).
- [28] R. Barth *et al.*, *GSI Annual Report* 1995, p. 51.
- [29] P. Senger, *this volume*.
- [30] A. Lang, W. Cassing, U. Mosel, and K. Weber, *Nucl. Phys. A* 541, 507 (1992).
- [31] T. Maruyama, W. Cassing, U. Mosel *et al.*, *Nucl. Phys. A* 573, 653 (1994).
- [32] W. Cassing, V. Metag, U. Mosel, and K. Niita, *Phys. Rep.* 188, 363 (1990).
- [33] W. Cassing, G. Batko, U. Mosel *et al.*, *Phys. Lett. B* 238, 25 (1990).
- [34] J. Aichelin and C. M. Ko, *Phys. Rev. Lett.* 55, 2661 (1985).
- [35] A. Schröter *et al.*, *Z. Phys. A* 350, 101 (1994).
- [36] P. Senger, to appear in *APH N.S., Heavy Ion Physics* (1996).

- [37] G. Q. Li, C. M. Ko, and X. S. Fang, *Phys. Lett. B* 329, 149 (1994).
- [38] J. Stachel and G. R. Young, *Annu. Rev. Nucl. Part. Sci.* 42, 537 (1992).
- [39] P. Braun-Munzinger *et al.*, *Phys. Lett. B* 344, 53 (1995).
- [40] M. Gonin *et al.*, *Phys. Rev. C* 51, 310 (1995).
- [41] G. Roche *et al.*, *Phys. Rev. Lett.* 61, 1069 (1988).
- [42] C. Naudet *et al.*, *Phys. Rev. Lett.* 62, 2652 (1989).
- [43] G. Roche *et al.*, *Phys. Lett. B* 226, 228 (1989).
- [44] G. Agakichiev *et al.*, *Phys. Rev. Lett.* 75, 1272 (1995).
- [45] M. A. Mazzoni, *Nucl. Phys. A* 566, 95c (1994); M. Masera, *Nucl. Phys. A* 590, 93c (1995).
- [46] T. Akesson *et al.*, *Z. Phys. C* 68, 47 (1995).
- [47] C. Baglin *et al.*, NA38, *Phys. Lett. B* 220, 471 (1989); B 251, 465 (1990).
- [48] M. Gonin *et al.*, NA50, QUARK MATTER '96, Heidelberg, May 1996, ed. P. Braun-Munzinger *et al.*, to appear in *Nucl. Phys. A*.
- [49] Gy. Wolf, G. Batko, W. Cassing *et al.*, *Nucl. Phys. A* 517, 615 (1990).
- [50] P. Koch, *Phys. Lett. B* 288, 187 (1992).
- [51] G. Q. Li, C. M. Ko and G. E. Brown, *Phys. Rev. Lett.* 75, 4007 (1995).
- [52] W. Cassing, W. Ehehalt, and C. M. Ko, *Phys. Lett. B* 363, 35 (1995).
- [53] M. Herrmann, B. Friman, and W. Nörenberg, *Nucl. Phys. A* 560, 411 (1993).
- [54] W. Cassing, W. Ehehalt, and I. Kralik, *Phys. Lett. B* 377, 5 (1996).
- [55] T. Ulrich *et al.*, QUARK MATTER '96, Heidelberg, May 1996, ed. P. Braun-Munzinger *et al.*, to appear in *Nucl. Phys. A*.
- [56] C. Hartnack *et al.*, *Nucl. Phys. A* 580, 643 (1994).
- [57] S. A. Bass, C. Hartnack, H. Stöcker, W. Greiner, *Phys. Rev. C* 51, 12 (1995).
- [58] B. Friman, QUARK MATTER '96, Heidelberg, May 1996, ed. P. Braun-Munzinger *et al.*, to appear in *Nucl. Phys. A*.
- [59] Ye. S. Golubeva, W. Cassing, A. S. Iljinov, and L. A. Kondratyuk, *preprint* UGI-96-26.